Hydrology Research

Hydrology Research Vol 52 No 6, 1223 doi: 10.2166/nh.2021.023

Large broad-leaved canopy of banana (*Musa nana* Lour.) induces dramatically high spatial–temporal variability of throughfall

Wanjun Zhang[a,b,c], Xiai Zhu[a,b], Chunfeng Chen[a,b], Huanhuan Zeng[a,b,c], Xiaojin Jiang[a,b], Junen Wu[a,b], Xin Zou[a,b,c], Bin Yang[a,b] and Wenjie Liu[a,b,*]

[a] CAS Key Laboratory of Tropical Forest Ecology, Xishuangbanna Tropical Botanical Garden, Chinese Academy of Sciences, Menglun, Yunnan 666303, China
[b] Center of Plant Ecology, Core Botanical Gardens, Chinese Academy of Sciences, Menglun, Yunnan, 666303, China
[c] University of Chinese Academy of Sciences, Beijing 100049, China
*Corresponding author. E-mail: lwj@xtbg.org.cn

WZ, 0000-0001-5274-5360

ABSTRACT

Throughfall (TF) is an important water input of rainfall redistribution into floor, and its spatial–temporal variability under some species' canopies has been documented to evaluate effect on splash erosion. However, the understanding of TF variability under large broad-leaved canopy remains insufficient. In this study, the spatial heterogeneity, temporal stability and drop size of TF were quantified using variogram fitting, normalised ranking and filter paper staining, respectively, under banana (*Musa nana* Lour.) canopy comprising long and wide leaves. Results indicated TF pattern showed strong spatial correlation at a range of 3–5 m. High spatial variability of TF was found, which was affected by rainfall event size and was accompanied by great canopy disturbance. TF plots revealed high time variability, which was mainly controlled by unstable banana canopy structure. TF drop size from leaf dripping points varied in 3–10 mm and showed significant differences ($p < 0.05$) among five kinds of leaf shapes, implying that concave and broken banana leaves were involved in the variability of TF drop size. Overall, results demonstrate the spatial–temporal variability of TF is dramatically induced by banana canopy with broad leaves, which may result in non-uniform soil water content and splash erosion under the canopy.

Key words: drop size, large broad-leaved canopy, spatial variability, temporal stability, throughfall

HIGHLIGHTS

- The specific banana canopy notably modifies spatial-temporal variability of throughfall.
- The spatial variability of throughfall was high and correlated with the rainfall event size.
- The spatial pattern of throughfall showed low time stability based on multi-temporal levels.
- Drop size of throughfall at different leaf shapes showed variable distribution in 3–10 mm.

INTRODUCTION

Throughfall (TF) is a critical component of rainfall redistribution, averagely contributing approximately four-fifths of gross rainfall into floor (Crockford & Richardson 2000; Levia & Frost 2006). Banana (*Musa nana* Lour.) plantations are widely cultivated in tropical and subtropical areas, where rainfall rates are high. The large broad-leaved canopy and abundant rainfall input dramatically modify the TF pattern under the banana canopy (Bassette & Bussière 2005). Considerable TF volume is generated at some dripping areas, six times greater than the incident rainfall rate under the banana canopy (Cattan *et al.* 2007; Yang *et al.* 2020). However, previous studies did not discuss TF variability in space and time scales in banana plantations, leaving some eco-hydrological problems unexplained, such as the reasons for heterogeneous soil water distribution and surface runoff rate (Klos *et al.* 2014; Zhu *et al.* 2021). Therefore, a thorough understanding of spatial–temporal variability of TF is essential in banana plantations (Yang *et al.* 2020).

The spatial heterogeneity of TF differs depending on the canopy structure (Staelens *et al.* 2006; Liu *et al.* 2019). For example, great TF volume appears in leaf dripping for the funnelling effect, and low TF volume appears for the shading effect (Germer *et al.* 2006). Some studies found that TF volume is related to the distance from tree trunks, e.g., greater

TF either at crown edges (André *et al.* 2011) or near the trunk (Fan *et al.* 2015), but other studies found no such relation (Carlyle-Moses *et al.* 2004; Kowalska *et al.* 2016). Moreover, TF shows a consistent spatial pattern in high rainfall events and inconsistent spatial pattern in low rainfall events; this phenomenon can be attributed to the relatively large canopy interaction for small rainfall amounts and satisfied canopy water storage capacity for large rainfall amounts (Keim & Link 2018). Such spatial variability with increasing rainfall amount has been consistently documented in different forest systems, such as in shrub stands (Zhang *et al.* 2016), oak stands (Rodrigo & Ávila 2001), beech stand (Dezhban *et al.* 2019) and Douglas fir stands (Bouten *et al.* 1992). Nevertheless, these forest types still show different degrees of spatial variability of TF because of their different canopy structures and rainfall parameters. Therefore, further study of TF in various canopy types or typical climate regions is important to gain further insight into the spatial heterogeneity of TF (Levia *et al.* 2019).

In addition to spatial variability, the ranked plots of TF volume were used to assess the temporal variability of TF patterns over rainfall events (Keim *et al.* 2005; Liu *et al.* 2019). Generally, TF is characterised by a temporally variable pattern, considering that canopies are considerably diverse in terms of species and/or event scale. For instance, TF in a mature Japanese cypress (*Chamaecyparis obtusa*) stand was proved to have a slightly temporal stability because of canopy change (Sun *et al.* 2015). Differently, several studies reported that the TF pattern is characterised by considerable time stability related to stable canopy structure (Wullaert *et al.* 2009; Zheng *et al.* 2019). Sato *et al.* (2011) noted that a high temporal stability with the persistence of very wet positions in a eucalyptus plantation was related to the canopy persistently manifesting a funnel effect on TF. If spatially heterogeneous water inputs are temporally stable over a long time, the spatial distribution of soil water and solute deposition would be affected in the long term (Klos *et al.* 2014; Zheng *et al.* 2019). Therefore, a deep understanding of the temporal stability of TF patterns is crucial to estimate the ecological consequence of water input into floor.

Banana plantations are largely developed in the tropics and subtropics around the world, e.g., Central America, Asia and Africa. In China, banana plantations cover 331,900 ha, accounting for over 6% of the total banana plantation area of the world (CSY 2018). However, the abnormal ecological environment caused by large-scale banana cultivation induced Fusarium wilt and nematodes, resulting in yield loss (Almeida *et al.* 2018). The eco-hydrological problems (e.g., water and soil loss) of banana plantations have received minimal attention. In order to delve into the hydrological process of banana plantations, our team has carried out some substantial studies over the past few years. Fortunately, several insights have been gained, including the basic characteristics of TF volume and TF kinetic energy in banana plantations (Harris 1997; Zhang *et al.* 2021), runoff affected by rainfall redistribution (Cattan *et al.* 2009) and the efficiency of water use in banana crops (Yang *et al.* 2020). However, many important questions remain unanswered, such as the spatio–temporal variability of TF and raindrop size. Understanding the spatial and temporal patterns of TF is necessary to optimise the management of banana plantations in terms of soil water and nutrition availability. Moreover, TF drop, generated by leaf dripping points, was different from open rainfall. In detail, larger TF drops were generated by rainfall drops coalescing on leaf surfaces and appeared to be of variable size distribution resulting from rainfall and leaf shape (Brandt 1989; Nanko *et al.* 2006). Understanding the distribution of TF drop size would help in assessing soil splash erosion (Levia *et al.* 2019). Therefore, this study focused on the spatial heterogeneity, temporal stability and drop size of TF to integrate the hydrological process of banana plantations. The objectives of this study are to: (1) quantify the spatial heterogeneity of TF under banana canopy using variogram method; (2) identify the time stability of the TF patterns by several temporal levels; and (3) estimate TF drop size by using the filter paper technique.

MATERIALS AND METHODS

Study site

The study site is located in Xishuangbanna Tropical Botanical Gardens (XTBG, 21.93° N, 101.27° E, 570–600 m a.s.l.), Yunnan Province, Southwest China. The local climate is dominated by a southwest monsoon carrying Indian Ocean moisture, and XTBG generates an apparent dry–wet season, including a rainy season from May to October and a dry season from November to April. According to the climate over the past 40 years, the mean annual air temperature and precipitation were 21.7 °C and 1,480 mm, respectively; approximately 87% of the annual total precipitation occurs during the rainy season (May to October) and 13% during the dry season (November to April) (Liu *et al.* 2016).

The study was conducted in a 4.3-ha banana plantation comprising a banana monoculture planted at a density of 5,000/ha (tree spacing 2×2 m). The stand characteristic was surveyed through 20 banana plants. In detail, the mean height of the mature banana plants was 295.1 cm, the mean basal area was 297.0 cm^2, the mean diameter at breast height was 18.7 cm, and the mean leaf area index (LAI) was 3.7. Mature banana bunches were harvested between April and May at three growth stages: vegetative, flowering and bunch appearance. After harvest, the pseudostem was chopped down and the new banana seedlings that sprouted from bulbs grew rapidly. The banana plantation was properly irrigated to meet the demand for water during the dry season, and was supplied by rainfall during the rainy season. The banana plantation was managed through the frequent application of fertilisers (10–15 times a year) near the root of each plant, and regular weeding and pest control (pesticide spraying) were performed throughout the year.

Data collection

Rainfall and TF samples were collected from June to September 2019. Rainfall was collected using a tipping-bucket rain gauge (3554WD, Spectrum Technologies Inc., USA), which was installed in an open field adjacent to the banana plantation at a distance of about 300 m. Rainfall data were recorded using a data logger (Model 115, Spectrum Technologies Inc., USA). The resolution of the rain gauge was ± 0.2 mm, and the time interval of data recording was set to 10 min.

TF was collected using an artificial funnel-type collector, comprising a short-stemmed funnel (6.0 cm in diameter) and a polyethylene bottle (1 L in volume). Further, 32 collectors were installed under the banana plantation canopy, wherein each collector was located column-wise in the middle of two plants. The plot area was $8 \text{ m} \times 16 \text{ m}$ with eight rows (1–8) and four columns (A–D) at 2-m spacing. Moreover, three replications (open rainfall) were performed as control-experiment in the open field, 20 m from the banana field. TF volume (mm) was acquired from the water volume of the bottle divided by the horizontal cross-sectional area of the funnel.

The drop size distribution of TF at the dripping points was measured using filter paper staining (Brandt 1989). Dye composed of eosin and talc with a weight ratio of 1:10 was evenly coated on the filter paper of 20 cm diameter. The leaf shapes at the dripping points were classified as valley, overlap, tip, breakage and complex shapes (Zhang *et al.* 2021). The pits on the leaf margin are uniformly defined as 'valleys' (Va) in our study. The 'overlap' (Ov) of concave areas sometimes appears where raindrops are intercepted by the upper leaf, then accepted by the lower leaf and finally drained away. In fact, the Va and Ov shapes are both microcatchments on the leaves. Moreover, the leaf 'tip' (Ti) and the 'breakage' (Br) approximate the triangular geometrical morphology, in which the water is intercepted and drained away based on the slope. Finally, we classified leaves at canopy drip points into four shapes: Va, Ov, Ti and Br. Moreover, some leaf shapes such as Va–Ov, Ov–Br, Va–Br and even Va–Ov–Br were also observed, and we uniformly defined them as complex shapes (Cs). In this study, five leaves per shape and two replications per leaf were prepared. A device of artificial rainfall was used with steady spray intensity. Artificial rainfall was continuously applied. The filter paper was quickly moved to the ground point where the raindrop was falling; when caught in the raindrops, the filter paper was pulled out quickly to prevent overlap raindrop stains.

In addition, the leaf area index (LAI) of the banana canopy structure was measured using a LAI-2200 plant canopy analyser with 90° view caps (Li-Cor Inc., USA). LAI values were determined above every TF position once a month (four times in all).

Throughfall-related analysis

TF variability is dependent on rainfall event size (Gómez *et al.* 2002). To analyse TF variability systematically, we built a suitable TF classification based on certain parameters via Spearman rank correlation analysis and Pearson correlation analysis (Table 1). The correlation coefficients related to the gross rainfall and the peak 30 min rainfall intensity (I_{30}) showed significantly higher values than other parameters. Thus, gross rainfall and I_{30} were selected as the optimal abiotic parameters for TF classification. Thus, the recorded 24 rainfall events were classified by the rainfall amount (i.e., 0 to <5, 5 to <10, 10 to <20, 20 to <30, 30 to <50 and ≥ 50 mm) and by I_{30} (i.e., 0 to <5, 5 to <10, 10 to <15, 15 to <20 and ≥ 20 mm). The rainfall event classifications were further expressed as P1, P2, P3, P4 and P5 for the five gross rainfall classes and as I1, I2, I3, I4 and I5 for the five rainfall intensity classes. Descriptive statistics, including the accumulative TF and corresponding TF rate, coefficient of variation (*CV*, the standard deviation as a proportion of the mean), skewness and kurtosis, were calculated for all groups (Table 2).

Variogram is widely applied to quantify the spatial dependence among geographic elements (Isaaks & Scrivastava 1989). In this study, we calculated the variogram $\gamma(h)$ to analyse the spatial autocorrelation of TF observations in the banana plantation.

Table 1 | Spearman rank of correlation coefficients between the rainfall amount and intensity of rainfall events and Pearson correlation coefficients between rainfall parameters and throughfall (TF) characteristics

Spearman	Gr	I_{10}	I_{20}	I_{30}	Ave. I
Gr		0.647**	0.715***	0.828***	0.307
I_{10}			0.856***	0.937***	0.794***
I_{20}				0.892***	0.645**
I_{30}					0.662***
I_{60}					0.677***
Pearson					
TF	0.990***	0.611**	0.743***	0.767***	0.072

Note: Gr, gross rainfall (mm); I_{10}–I_{30}, peak 10, 20 and 30 min rainfall intensity (mm 10 min^{-1}, mm 20 min^{-1} and mm 30 min^{-1}); Ave. I, mean rainfall amount per hour (mm h^{-1}); ***$p < 0.001$, **$p < 0.01$, *$p < 0.05$.

Table 2 | Descriptive statistic of cumulative throughfall (TF) for total rainfall events and classified rainfall groups

Rainfall (mm)			TF (mm)			
	Events	Volume	Total (TF/GR)	*CV*	Skewness	Kurtosis
Total	24	626.3	508.7 (81.2%)	28.8%	0.16	−0.95
Rainfall (mm)						
P1 (0.9–5.9)	5	13.2	10.7 (81.1%)	22.3%	−0.69	0.00
P2 (10.6–14.5)	5	63.7	53.3 (83.7%)	30.5%	0.35	−1.18
P3 (16.5–20.2)	4	72.1	56.1 (77.7%)	34.5%	−0.83	0.55
P4 (33.7–42.6)	5	189.6	147.8 (77.9%)	15.8%	−0.33	−0.32
P5 (49.3–69.4)	5	287.2	240.7 (83.7%)	17.4%	−0.41	−1.00
I_{30} (mm 30 min^{-1})						
I1 (0.4–3.6)	6	37.7	32.2 (86.0%)	22.6%	0.11	−0.73
I2 (5.7–10.7)	6	101.5	83.3 (82.1%)	20.2%	0.21	−0.89
I3 (11.5–15.1)	5	167.5	134.3 (80.1%)	28.5%	−0.07	−1.04
I4(17.7–19.4)	3	105.4	82.4 (78.1%)	23.5%	0.32	−1.24
I5 (20.5–30.6)	4	214.2	176.5 (82.4%)	16.0%	−0.49	−0.26

Note: P1–P5, five groups classified by gross rainfall amount; I1–I5, five groups classified by the peak 30 min rainfall intensity.

The variogram $\gamma(h)$ was computed as follows:

$$\gamma(h) = \frac{1}{2n(h)} \sum_{i=1}^{n(h)} [z(x_i) - z(x_{i+h})]^2 \quad (1)$$

where $n(h)$ is the number of sample pairs, and the index i is the different spatial location of the samples. The values of samples $z(x_i)$ and $z(x_{i+h})$ at two positions x_i and x_{i+h} are separated by the lag distance h. An appropriate semivariogram for the cumulative TF is computed by adjusting active lag distances until the minimum residual sum of squares (*RSS*) and the maximum coefficient of determination (r^2) appeared. The spatial autocorrelation is evaluated by the parameters of the model, nugget (C_0), sill ($C + C_0$), partial sill (C). Relatively strong autocorrelation structure is defined by the partial sill/sill >75%; somewhat weak autocorrelation structure is defined by the partial sill/sill <75%; the partial sill/sill close to 0% features a pure nugget structure and displays no spatial correlation (Keim *et al.* 2005). The fractal dimension, which is defined as the slope of $\gamma(h)$,

is used to ascertain the degree of spatial heterogeneity in different directions. The fractal dimension (D) was calculated as follows:

$$2\gamma(h) = h(4 - 2D) \tag{2}$$

$$D = (4 - m)/2 \tag{3}$$

where m is the slope of linear regression. The values of D were computed in four directions: 0° (east–west), 45° (northeast–southwest), 90° (south–north) and 135° (northwest–southeast).

To quantify the temporal persistence of the spatial distribution of TF, we normalised the TF volume by using the following equation from Keim *et al.* (2005):

$$\tilde{T}_{ij} = \frac{T_{ij} - \bar{T}_j}{SD_j} \tag{4}$$

where $\bar{T}_{ij}$ is the normalised TF at sampling point i for event j, T_{ij} is the TF at sampling point i for event j and $\bar{T}_j$ and SD_j are the mean TF and standard deviation of the TF during that rainfall event, respectively. The normalised TF was ranked from minimum to maximum. This type of graph explained two types of temporal stability. First, the extreme persistence was defined as a large deviation of the normalised TF in the lower and upper quartiles of the arranged positions, where the sites are persistently very wet or dry at steeply sloping tails of the ranked line. Second, the general persistence was defined as a general deviation of the normalised TF in the interquartile range, where the sites are persistently wetter or drier than the mean TF (Keim *et al.* 2005).

For the drop size experiment, after allowing drying naturally, the filter paper was scanned with 1:1 into the computer and the stain diameter was calculated by software Image J. Previous studies have documented that a good correlation between stain diameter and raindrop diameter was found (Dou & Zhou 1982; Xu *et al.* 2004; Lu *et al.* 2015). Zhu *et al.* (2014) once studied the drop size distribution in this region and built an appropriate relation between stain diameter and raindrop diameter. Thus, the TF drop size diameter in this study was calculated using the following formula built by Zhu *et al.* (2014):

$$d = 0.3684 \times D^{0.7093} (R^2 = 0.9988) \tag{5}$$

where d is the actual drop size diameter (mm), and D is the diameter of stains on the filter paper (mm). The stain diameters for the drop size experiment were measured using Image-J software.

Statistical analysis and calculations

The normality of TF was tested by using the Kolmogorov–Smirnov test. A log-transformation or square root transformation was conducted for non-normally distributed data. The variograms of TF in different categories were calculated using GS + 9.0 (Gamma Design Software). The differences in TF drop size among different leaf shapes were assessed using one-way analysis of variance (ANOVA), followed by a Tukey test for multiple comparisons between means. Spearman rank of correlation coefficients and Pearson's coefficients were used to test for linear correlations between the variables. All statistical procedures were conducted with $\alpha = 0.05$ threshold for significance, in the IBM SPSS statistics 22.0 software (IBM Inc.).

RESULTS

Rainfall and throughfall quantity

The total rainfall was 832.6 mm during the study period of 2019, which was lower than the annual mean value over the past decade (2009–2018) (Figure 1). The rainfall amount in the rainy season accounted for 77.4% of the total annual rainfall, similar to the annual record over the past decade. A total rainfall amount of 626.3 mm was collected for 24 rainfall events (0.9–69.7 mm) during the TF sampling period, with approximately 75.2% of the annual rainfall. The cumulative TF volume was 508.7 mm, on average 81.2% of the gross rainfall in the sampled banana plantation (Table 2). Moreover, descriptive statistics for each classified group showed that TF rate ranged within 77–86%, skewness −0.69–0.35 and kurtosis −1.18–0.55.

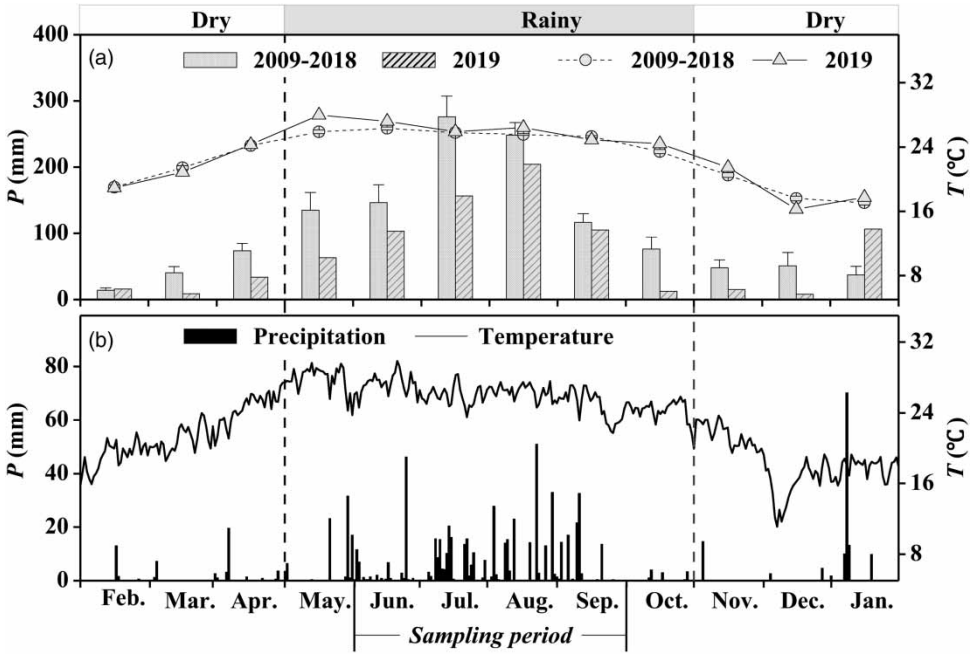

Figure 1 | (a) Monthly mean precipitation and air temperature in 2009–2018 and 2019, respectively. (b) Daily precipitation and air temperature in 2019 for the study period. Weather data were obtained from the Xishuangbanna Station for Tropical Rainforest Ecosystem that is adjacent to the study site. Error bars represent ± standard error (SE).

Spatial heterogeneity of throughfall

The spatial distribution of TF is heterogeneous for rainfall events (Figure 2). The number of wetter TF collectors beyond open rainfall increased with increasing rainfall volume and rainfall intensity. The distribution patterns of high-value areas and low-value areas were significantly different in rainfall groups, and there were more high-value points under heavy rainfall events (e.g., P4, P5, I4 and I5) than those under smaller rainfall events (e.g., P1, P2 and I1). For the spatial correlation, the best-fitting theoretical models for the TF semivariance via rainfall classification are shown in Figure 3. The fractural D values showed zonal anisotropy in different directions; therefore, the theoretical models were fitted. Some differences in the variogram results were found among different rainfall event classification (Table 3). In particular, in the gross rainfall classification, a spherical model fitted for two events (i.e., P1 and P2) showed a nearly stable sill in the range of 4–5 m (4.47 m and 4.34 m, respectively). Two events (i.e., P3 and P4) were fitted with a linear model, indicating an unclear stable sill. P5 was fitted with an exponential model for a nearly stable sill at the range of 3.3 m. By contrast, TF variance was fitted with higher proportions (>75%) in the P1, P2 and P5 groups compared with the P3 and P4 groups. In the rainfall intensity (I_{30}) classification, a spherical model and an exponential model best-fitted for two events (i.e., I1 and I5, respectively) showed a nearly stable sill in the range of 4–5 m. TF for I4 was fitted with an exponential model for weak correlation. However, the other events (i.e., I2 and I3) were fitted with a linear model, suggesting unclear stable sills and low proportions (both 0%).

The *CV*s of TF are scattered with gross rainfall and I_{30} in Figure 4. TF in the banana plantation showed spatial variability mostly with *CV*s > 20%, especially at some points >50%. Notably, the *CV*s of TF varied with increasing gross rainfall and I_{30}, but extremely weak nonlinear relationships were fitted between *CV*s and gross rainfall and I_{30}. Thus, their relationships were fitted by partitioning two different zones (small and heavy rainfall events). The *CV*s significantly decreased by exponential function for both zones ($R^2 > 0.5$, $p < 0.001$) (Figure 4(a)). In the transitional zone (green pane filled with dots), decreasing *CV*s for small rainfall events (<15 mm) increased, and then high *CV*s decreased again with increasing gross rainfall for events >30 mm. In addition, the *CV*s significantly decreased with I_{30} by exponential function for both zones ($R^2 > 0.6$, $p < 0.001$) (Figure 4(b)). Meanwhile, the transitional zone ranged from 10 mm 30 min^{-1} to 15 mm 30 min^{-1}. In addition, in different classifications for each group, the *CV*s ranged from 16% to 35% (Table 2). Meanwhile, the *CV*s initially increased and then decreased from P1 (and I1) group to P5 (and I5) group, with peak values appearing for the moderate rainfall events

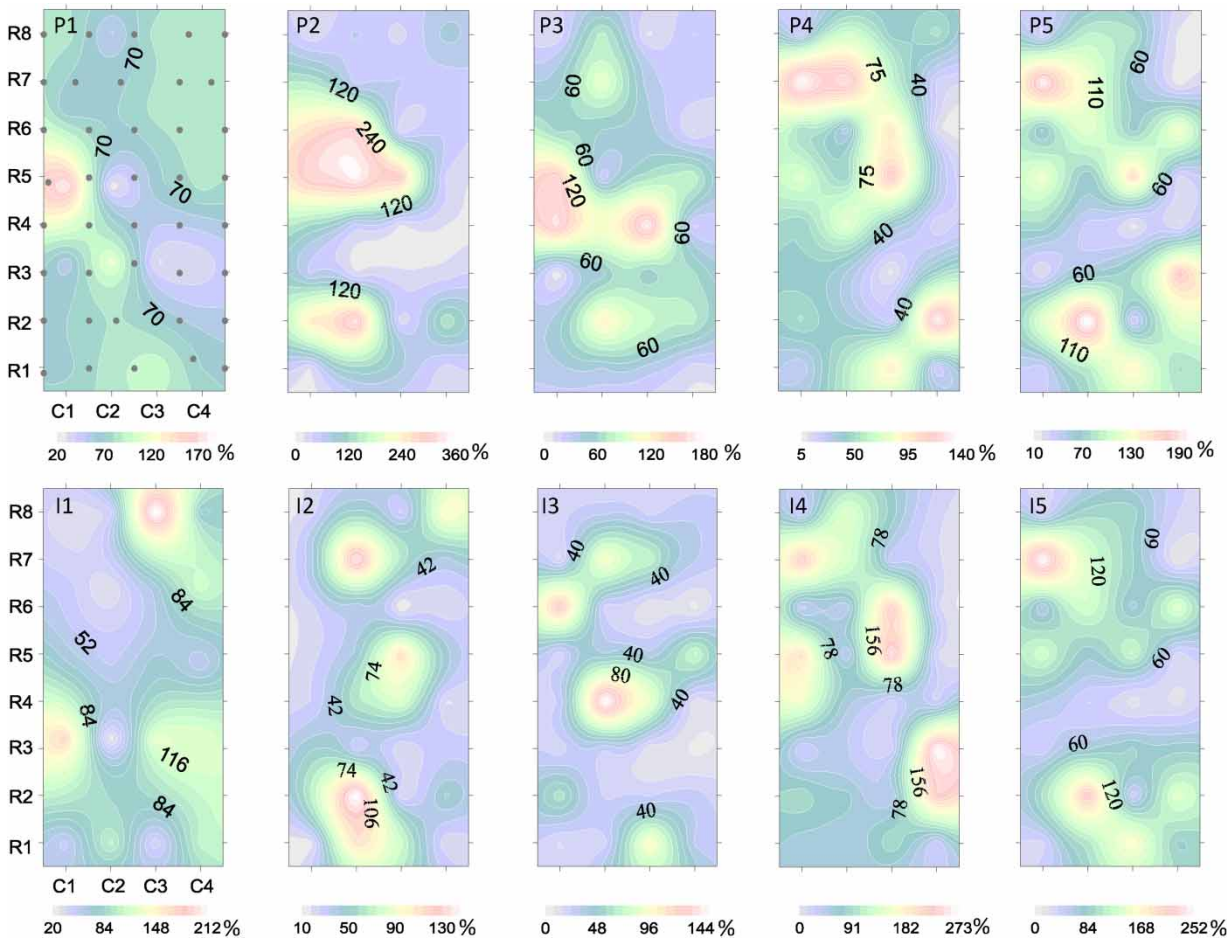

Figure 2 | Spatial distribution of throughfall ratio for classified rainfall groups. The solid black dots indicate the locations of the banana trees, and the horizontal and vertical coordinates (C, R) indicate the location of the throughfall collectors, 32 collectors in total. P1–P5 indicates the five groups classified by gross rainfall, and I1–I5 indicates the five groups classified by peak 30 min rainfall intensity.

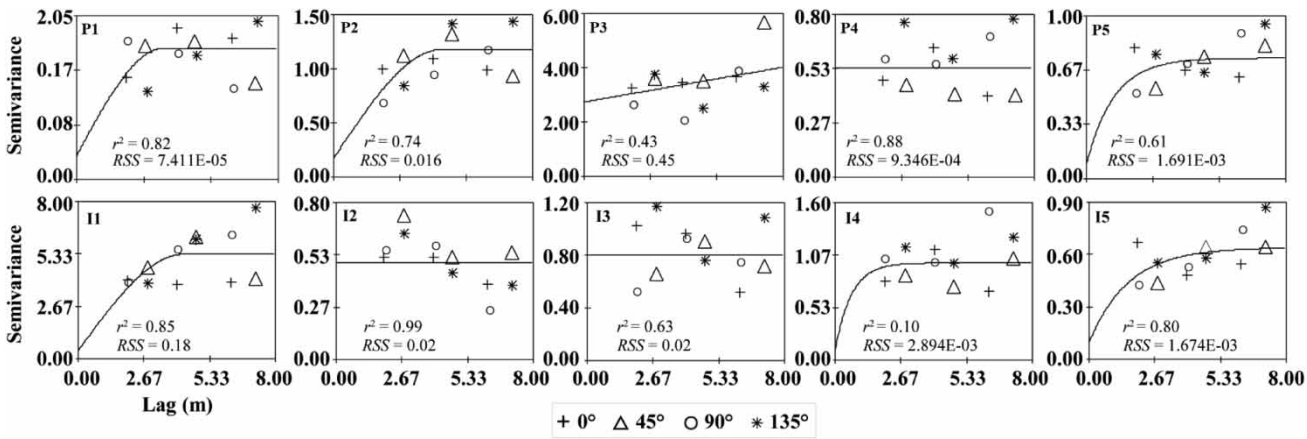

Figure 3 | Experimental anisotropic semivariograms for throughfall and fitted models in multiple directions for rainfall groups. P1–P5 indicates the five groups classified by gross rainfall. I1–I5 indicates the five groups classified by peak 30 min rainfall intensity. Result from 0°, 45°, 90° and 135° indicate the anisotropic semivariograms for throughfall at four directions.

(i.e., P3 and I3 groups). The spatial distribution of TF showed a higher variability in the P3 group, with a *CV* of 34.5%, than those in other groups. Similar results of TF variability were also found in I_{30} classifications for each group.

Table 3 | Characteristics of isotropic variogram models in different groups classified by gross rainfall and rainfall intensity (I_{30})

Events	Model (A)	Nugget	Sill	r^2	RSS*	C/(C + C$_0$)
Total	Exp. (4.29)	0.05	0.38	0.38	2.422×10^{-3}	0.86
Rainfall						
P1	Sph. (4.47)	0.04	0.30	0.85	6.160×10^{-4}	0.86
P2	Sph. (4.34)	0.17	1.17	0.74	0.016	0.86
P3	Lin. (–)	2.69	3.74	0.43	0.45	0.28
P4	Lin. (–)	0.53	–	0.88	9.346×10^{-4}	0.00
P5	Exp. (3.30)	0.08	0.73	0.61	1.691×10^{-3}	0.89
I_{30}						
I1	Sph. (4.28)	0.47	5.39	0.85	0.18	0.91
I2	Lin. (–)	0.50	–	0.99	0.02	0.00
I3	Lin. (–)	0.80	–	0.63	0.02	0.00
I4	Exp. (1.95)	0.09	0.98	0.10	2.894×10^{-3}	0.90
I5	Exp. (4.8)	0.096	0.65	0.80	1.674×10^{-3}	0.85

Theoretical model, nugget, sill, R^2, RSS and ratio between partial sill and sill parameters to percentage can be seen.
Note: P1–P5, five groups classified by gross rainfall amount; I1–I5, five groups classified by the peak 30 min rainfall intensity.

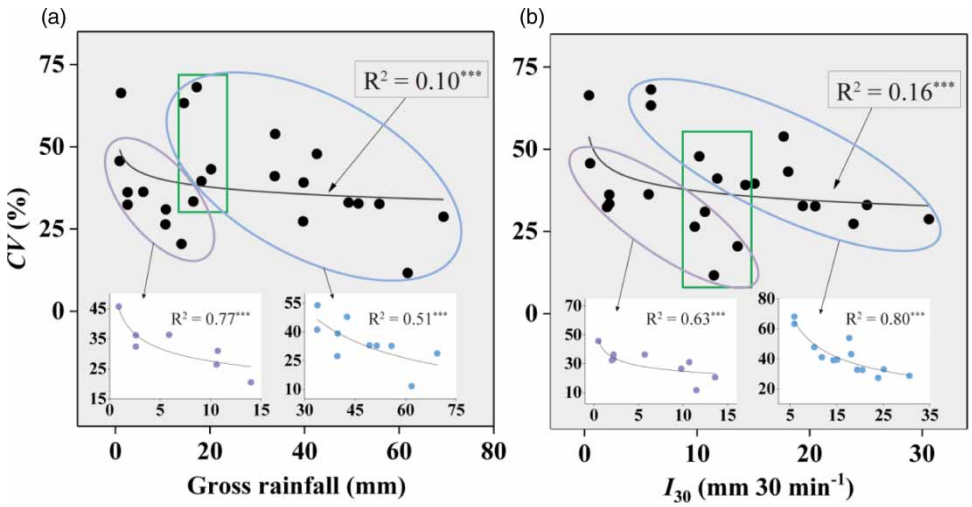

Figure 4 | Fitted trends in the coefficient of variation (*CV*) of throughfall varying with increasing gross rainfall and peak 30 min rainfall intensity (I_{30}). R^2 (correlation coefficient) showed significant probability (p). *** denotes $p < 0.001$. Please refer to the online version of this paper to see this figure in colour: http://dx.doi.10.2166/nh.2021.023.

Temporal stability of throughfall

The temporal stability of spatial TF patterns in the banana plantation was studied at three temporal levels based on Spearman rank correlation. At the first temporal level, relationships among the cumulative TF volumes across different rainfall classes P1–P5 were determined (Table 4). The significant correlation ($p < 0.05$) among the cumulative TF volumes per rainfall class was not fully determined and was found only in P2, P4 and P5. At the second temporal level, relationships among the monthly cumulative TF volumes across four months (June–September) were determined. The monthly cumulative TF volumes showed no significant or strong correlation, except the correlation between August and September ($r = 0.37$, $p < 0.05$). At the third temporal level, the correlations with each other of the TF volumes for all rainfall events were calculated, and a significant ($p < 0.05$, $n = 32$) positive Spearman correlation coefficient was found for 10.9% of the pairs of events (numbers of pairs of 24 rainfall events = 276) (Table 4).

Table 4 | Spearman rank of correlation coefficients between the cumulative throughfall of rainfall events within five rainfall classes under the banana canopy

Rainfall groups	P1	P2	P3	P4	P5
P1	1	0.084	0.222	−0.03	−0.125
P2		1	0.147	0.467**	0.523**
P3			1	0.337	0.206
P4				1	0.409*
P5					1
Months	**June**	**July**	**August**	**September**	
June	1	0.23	0.068	0.147	
July		1	0.164	0.328	
August			1	0.373*	
September				1	
Time-stable pairs of events (%)	10.9%[a]				

Note: P1–P5, five groups classified by gross rainfall; ***$p < 0.001$, **$p < 0.01$, *$p < 0.05$.

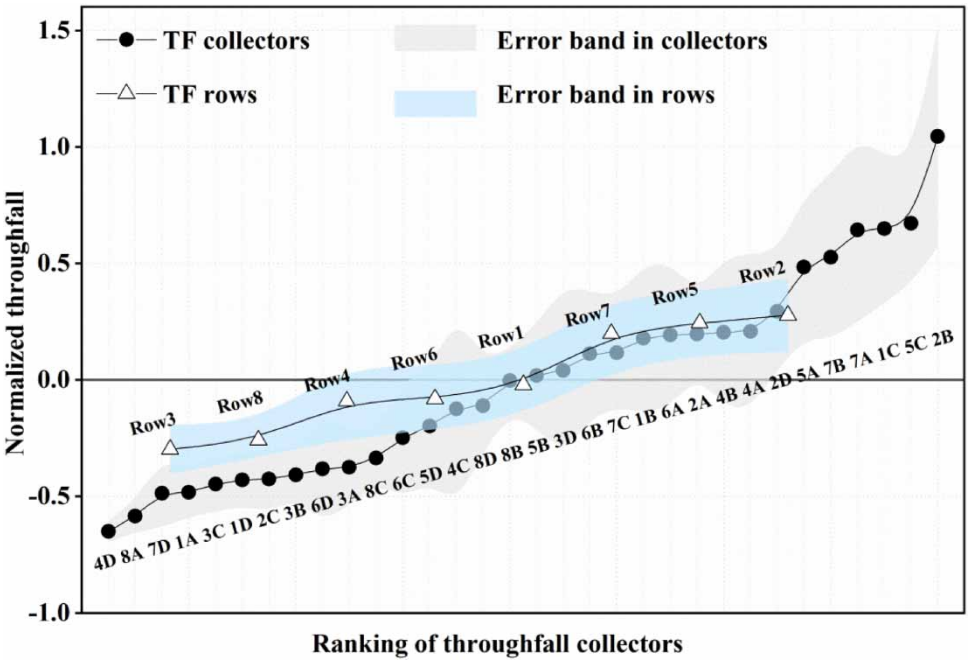

Figure 5 | Time stability plots of normalised throughfall to zero mean at unit variance and in each row are shown for total event. Thirty-two plots consist of eight rows (1–8) and four columns (A–D) of TF collectors. The number–letter names (row–column) of the TF collectors below the figure are ranked by their means in the plot. Error bands represent ± SE.

In addition, the temporal stability plots for the mean normalised TF in each collector position and for different rows are shown in Figure 5. For total rainfall events, the mean normalised TF was significantly different than zero for 34.4% of the samples (t-test; $\alpha = 0.05$). No TF collectors were very dry, and a tail indicated persistence of individually wetter TF collectors, showing moderate general persistence in the stand. For each row, a moderate general persistence was also found, with no rows that were extremely wet or dry. Moreover, each plot of four months was ranked in ascending order (Figure 6), and results showed that TF was characterised by great general persistence, particularly the persistence of extremely dry collectors (e.g., 3C, 6C, 7D and 7D corresponding to June, July, August and September, respectively) and few very wet collectors (e.g., 1B, 2B, 7A and 4A corresponding to June, July, August and September, respectively).

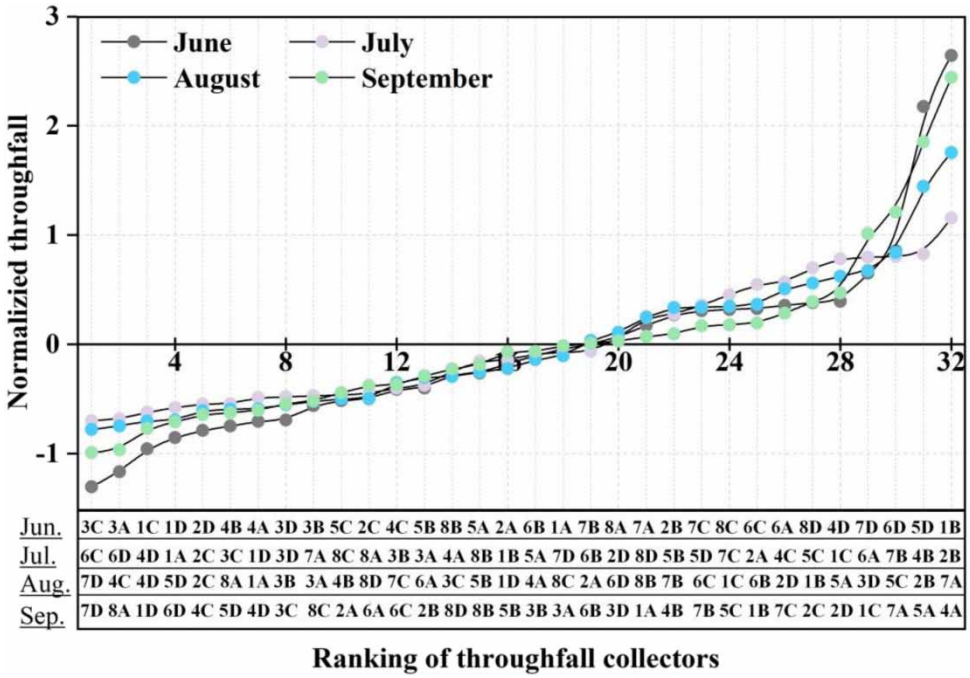

Figure 6 | Time stability plots of normalised throughfall to zero mean are shown in the months June–September. Thirty-two plots consist of eight rows (1–8) and four columns (A–D) of TF collectors. The number–letter names (row–column) of the TF collectors below the figure are ranked by their means in the plot.

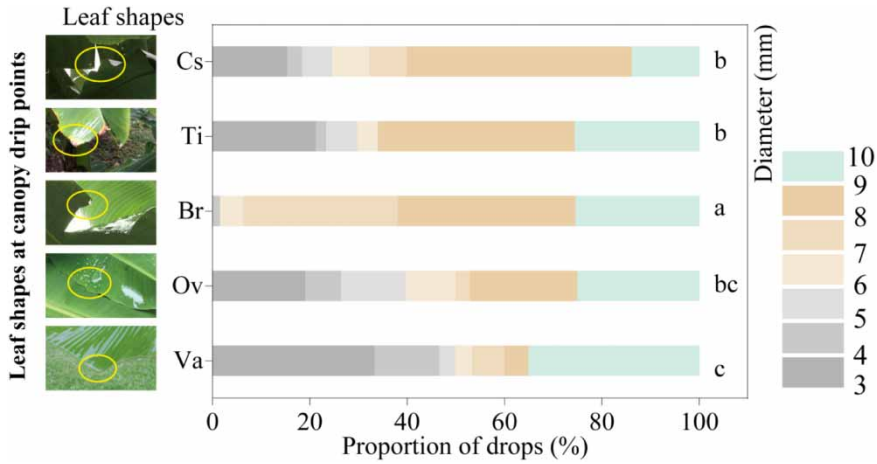

Figure 7 | Proportion of throughfall drop number in different drop size at each banana leaf shape. Va, Ov, Br, Ti and Cs indicate valley, overlap, breakage, tip and combined shape of banana canopy dripping points, respectively. Different lowercase letters (a, b and c) indicate significant difference at $p < 0.05$.

Drop size distribution of throughfall

The drop size of TF was in the range of 3–10 mm and was divided into different proportions in each leaf shape (Figure 7). For the Va shape, the number of TF drops in the range of 3–4 and 9–10 mm showed larger proportions of 33.3% and 35.0% of the number of total raindrops, respectively, than other drop sizes. The TF drop size for the Ov shape was mainly in the range of 8–10 mm, a proportion of 47.0%. A large proportion of drop size ranging from 7 to 10 mm was found for the Br shape, which accounted for 93.7% of the total drops. The TF drop size for the Ti shape was mainly in the range of 8–10 mm with a proportion of 80.0%. As for the Cs shape, a TF drop size of 8–9 mm showed a larger proportion of 46.1%, than other drop

sizes. In addition, a significant difference ($p < 0.05$) in TF drop size was found among the different leaf shapes. On average, the drop size of TF followed a decreasing order of Br > Ti > Cs > Ov > Va.

DISCUSSION

Comparison of spatial heterogeneity in throughfall

The spatial dependence of TF in a certain range reflected the spatial heterogeneity of TF because of the interaction of the surrounding TF plots (Gómez *et al.* 2002). In this study, the TF was spatially correlated up to a range of approximately 3–5 m and presented a strong autocorrelation structure. This suggested that a sampling distance could be considered >5 m in the banana plantation. Gómez *et al.* (2002) found a nearly stable sill at an approximated 1–3 m distance in isolated olive trees. Staelens *et al.* (2006) observed a slightly farther distance of 3–4 m under an individual deciduous beech tree and Fathizadeh *et al.* (2014) reported a significant farther range of approximately 5–6 m in oak (*Quercus brantii var. Persica*) trees, suggesting that larger sampling distance should be conducted in the oak trees. These differences in the spatial heterogeneity of TF are expected, and one reason is that the differences in canopy species, canopy structure (e.g., tree height, leaf area and LAI) and meteorological phenomena alter the spatial patterns of TF (Keim & Link 2018). The banana tree with about 3 m height is generally lower than most forest trees, and the banana leaf area (about 1.5 m^2 per leaf) is significantly larger than that of the common vegetation leaf, all of which cause the distinct different distribution pattern of TF. Another reason is that the choice of sampling schemes, such as area extent, sampling size and layout, has a substantial influence on the variogram results (Voss *et al.* 2016). Besides, groups P4, I2 and I3 had extremely small sill proportions (0.0%), displaying no spatial correlation. Similar to our finding, the spatial correlation of TF was absent in a maritime pine stand (Loustau *et al.* 1992) and in Mediterranean dry forest (Bellot & Escarre 1998). The variograms in the I2 and I3 groups did not reach a stable sill at a range possibly because of the high minimum intermediate distance between the TF collectors, resulting in a lack of information on the spatial correlation at a small distance (Fathizadeh *et al.* 2014).

The spatial variability of TF was verified to significantly decline with increasing rainfall amount in previous researches (Whelan & Anderson 1996; Fan *et al.* 2015). By contrast, our study found weak correlations between *CV*s and rainfall amount and I_{30} for the 24 monitored rainfall events (Figure 4). Fortunately, we found significant correlations when rainfall events were divided into two intervals, relatively low and high rainfall events, respectively. Results showed that two distinctly exponential trends were observed with increasing rainfall amount and intensity. The two forces from rainfall and canopy intensively counteract each other and induced such results. In particular, for small rainfall events, canopy interactions are relatively large, resulting in a high degree of spatial TF variability initially (Lin *et al.* 1997) and a strong correlation between *CV*s and rainfall amount. With the increase of rainfall amount, the splash intensity of dripping water on the leaves increases, which induces canopy shaking. The shaking canopy as well as the converging and shading effects of the leaves interfere with the falling pattern of raindrops. Thus, for the moderate rainfall events, the *CV*s were unsteady likely due to a transitional interaction between rainfall and canopy factors. For the high rainfall events (>30 mm), the *CV*s again declined with increasing rainfall amount. Moreover, the *CV*s in the P4, P5 and I5 groups were smaller than those in the other groups (Table 2), also indicating that a relatively low degree of TF spatial variability would be generated in high rainfall events. Similarly, previous studies also demonstrated that the spatial variability of TF was restricted by canopy complexity and rainfall depth (Lloyd & Marques 1988; Holwerda *et al.* 2006; Kowalska *et al.* 2016). Carlyle-Moses *et al.* (2004) noted that *CV* value decreased with increasing rainfall volume and afterwards remained quasi-constant after a rainfall threshold was reached. Their study suggested that the spatial distribution of TF volume was also determined by the distribution of canopy drip and shelter point locations. In banana plantations, unexceptionally, the spatial variability of TF can be attributed to these documented factors, rainfall and canopy structure. In summary, the increasing rainfall volume induced the decrease in TF spatial variability for the 24 monitored rainfall events. Considering the extremely long, wide banana leaves, the spatial distribution of TF was likely dependent on the banana canopy structure, particularly the dramatic variability in the TF volume due to the banana canopy funnelling and shading effects.

Temporal stability of throughfall patterns

In this study, the significant correlation of TF volume was not fully caught at the temporal levels based on Spearman rank correlation, indicating that TF pattern was inconsistent across rainfall events in the banana plantation. At the experiment scene, we noticed that the dry TF collectors were mostly adjacent to the shade of banana leaves, a few of which never received

any raindrops. The wet collectors were obviously related to the convergence effect of large banana leaves. In general, the shading and funnelling areas for the canopy were distributed at random. Thus, the case of persistently dry and/or wet TF in the same collectors rarely appeared across rainfall events. Moreover, the time stability of spatial TF pattern was lower (10.9%) at the level of individual rain events compared with the results (14.2%–28.8%) in individual oak trees (*Quercus brantii var. Persica*) reported by Fathizadeh *et al.* (2014). This difference suggests that the canopy factor control on TF variability may be more complex than the rainfall parameter control. In addition, the proportion of sampling points (approximately 34%) deviating consistently in two directions from the mean normalised TF in banana plantation was similar to the 31–46% detected in two coniferous forests and a deciduous forest (Keim *et al.* 2005) but higher than the 1.4%–5.2% found in Persian oak trees (*Quercus brantii var. Persica*) (Fathizadeh *et al.* 2014). Thus, our result illustrated that TF volumes at sampling points were not entirely randomly distributed over time, and the TF volume obviously showed a high temporal variability. Similarly, Germer *et al.* (2006) also reported a high temporal variability in an open tropical rain forest. However, there is no consistence among previous studies; for instance, Keim *et al.* (2005) found a low temporal variability for coniferous and deciduous stands. As described above, a possible explanation for the low temporal stability (namely, high temporal variability) of TF spatial pattern in our experiment should be attributed to frequent changes in canopy properties (Loescher *et al.* 2002).

In addition, the correlation coefficients among TF, GR and I_{30} for each TF plot were calculated to identify the effect of rainfall events on TF from 32 different collectors. Results showed that the quantity of collectors with significant correlation ($p < 0.05$) was obviously less than the collectors with weak and even no correlation (Supplementary Material, Figure S1). As previously stated, the differences among TF collectors in terms of the effect of rainfall characteristics are potentially a result of biotic factors, among which, canopy structure is a major contributing factor to rainfall redistribution (Zimmermann *et al.* 2007; André *et al.* 2011). LAI has been proved to exert an important effect on the TF variation of other forest systems (Song *et al.* 2018). In this study, LAI values under the banana canopy were measured to verify LAI's effect on TF variability. Unfortunately, significant correlation between TF volume and LAI was not found. The raindrop funnelling and shading areas for the canopy were distributed at random around the banana plantation, thus, not affected by the high or low LAI. In fact, the funnelling and shading areas of banana canopy are promoted by the leaf size, whose area is often up to 1.5 m^2, much greater than that of common tree leaves. Thus, the effect of the banana canopy on rainfall redistribution was different from that of other forest canopies (Staelens *et al.* 2006). Overall, the spatial–temporal variability of TF in the banana plantation showed peculiarity resulting from the large broad-leaved canopy.

Difference in throughfall drop size

In addition to promoting the pronounced spatial–temporal variability of TF, canopy effect on TF was also reflected in various components of TF drop size. In general, large TF drops are generated by rainfall drops coalescing on the leaf surfaces (Nanko *et al.* 2006). In the banana planation, the TF drop size distribution of 3–10 mm showed a great range of canopy drip. However, previous studies reported that the TF drop size distribution of canopy drip is mostly <7 mm (Hall 2003; Levia *et al.* 2019), which is significantly lower than the peak of banana canopy drip. Drop size of tall trees was found to be lower than that of short shrubs in Amazon forest systems, indicating that tree height was an essential factor affecting leaf drop size (Rebelo & Williamson 1996). Therefore, the result, relatively large drop size of banana leaf, can be attributed to relatively low height compared to tall trees. In addition, the large drop size (7–10 mm) of the banana canopy drip can be ascribed to the fact that the extremely large leaf size facilitated the coalescence of raindrops on the leaf surface. Such case is no exception, and some studies have indicated that the broad-leaved tree (or matte leaves) indeed could generate larger TF drop size than the coniferous tree (or coated leaves) (Nanko *et al.* 2006, 2013). Significant differences in TF drop size distribution were observed among different leaf shapes. This result indicated that the ability of the raindrops to coalesce in different leaf shapes might be a result of such significant differences. Accordingly, specific canopy with different leaf shapes could be considered as a key biotic factor affecting the TF volume and drop size distribution of certain species.

Implications

The spatially heterogeneous TF input produces wetter and drier soil areas within a short time (Zheng *et al.* 2019). Soil subsurface flow or rapid recharge to groundwater can be affected by soil surface water distribution (Weiler & Naef 2003). In the sampled banana plantation, the highly spatial variability of TF was detected. As a result, heterogeneous TF input is likely to produce extremely wet and extremely dry soil areas. Thus, whether or not the high spatial variability of TF contributes to some differences in soil water dynamics in the banana plantation is worthy of further study in future.

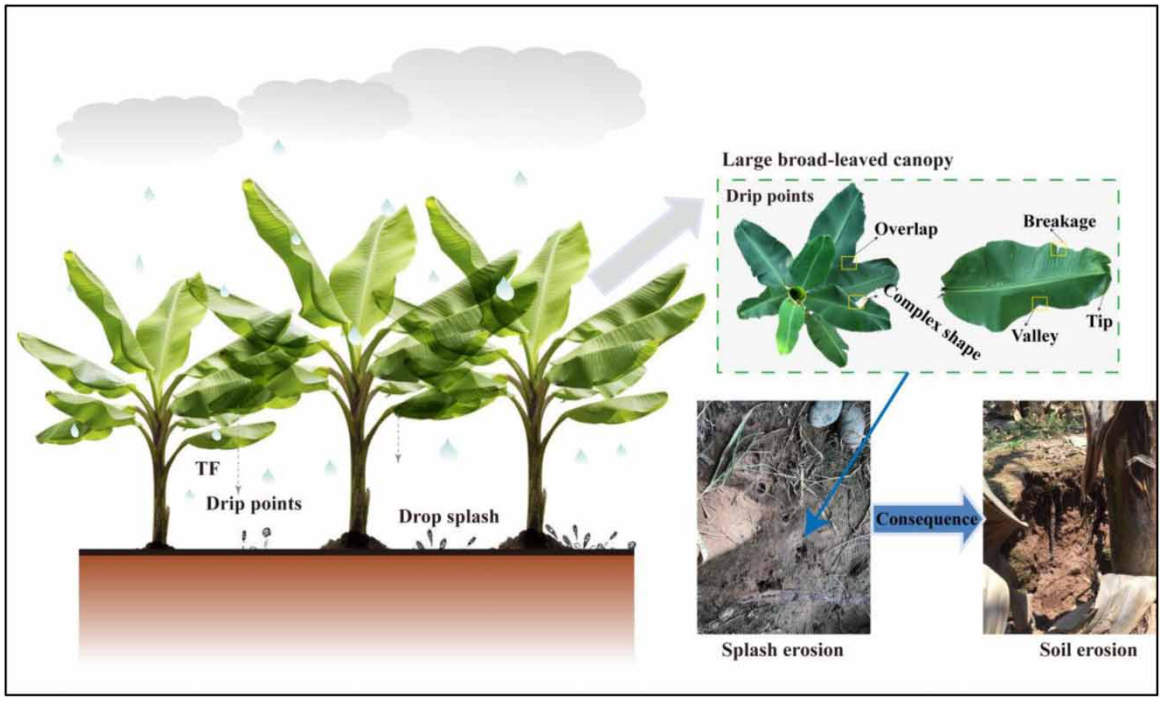

Figure 8 | Effects of large broad-leaved canopy on throughfall patterns in the banana plantations.

Heavy rainfall can provide abundant water for soil moisture and also leach canopy elements to soil solute concentrations. However, the negative effect is that heavy rainfall may generate serious water and soil loss via surface runoff. In our study site, soil erosion frequently occurs during the rainy season, which covers six months each year (Figure 8). The banana canopy converges raindrops and TF shows large temporal and spatial variability, which affects the soil splash erosion distribution. Some studies have reported that the TF splash erosion potential in agroforestry systems is significantly lower than that in monocultures because multiple-layered canopies can prevent the raindrop size and terminal velocity of intercropping plants (Zhu *et al.* 2018; Liu *et al.* 2018). In practice, the agroforestry ecosystem of multiple canopies can be considered instead of the monoculture banana plantation.

CONCLUSION

This study confirmed the spatial heterogeneity and temporal stability of TF for 24 rainfall events and the TF drop size in a banana plantation. The TF volume showed strong spatial correlation up to a range of approximately 3–5 m. The spatial pattern of TF maintained high variability, and the spatial variability twice exponentially declined with increasing rainfall amount in two separate rainfall intervals, respectively. This unusual trend can be attributed to the significant canopy effect against rainfall effect in different ranges of rainfall event size. Moreover, the observed spatial pattern of TF was temporally low and stable during the four months of observation, which was controlled by an unstable banana canopy structure. In addition, the TF drop size from the leaf dripping points varied highly in 3–10 mm and had significant differences ($p < 0.05$) among five types of leaf shapes. Thus, large broad-leaved canopy of banana can dramatically modify the spatial–temporal variability of TF.

ACKNOWLEDGEMENTS

The authors deeply appreciate two anonymous reviewers for their constructive comments. We also thank Mr Liu MN for his help in the field. We also thank the Xishuangbanna Station for Tropical Rainforest Ecosystem Studies and the Central Laboratory of XTBG for their help. This research was supported by the Natural Science Foundation of Yunnan Province (202101AS070010, 202101AT070056, 202001AU070136, 2018FB076 and 2018FB043), the National Natural Science Foundation of China (31570622 and 32001221), and the Youth Innovation Promotion Association CAS (2018430).

COMPETING FINANCIAL INTERESTS

The authors declare that they have no known competing financial interests or personal relationships that could have appeared to influence the work reported in this paper.

DATA AVAILABILITY STATEMENT

All relevant data are included in the paper or its Supplementary Information.

REFERENCES

Almeida, N. O., Teixeira, R. A., Carneiro, F. A., de Oliveira, C. M., Ribeiro, V. A. & Rocha, M. R. D. 2018 Occurrence and correlations of nematodes, Fusarium oxysporum and edaphic factors on banana plantations. *Journal of Phytopathology* **166** (4), 265–272. doi:10.1111/jph.12683.

André, F., Jonard, M., Jonard, F. & Ponette, Q. 2011 Spatial and temporal patterns of throughfall volume in a deciduous mixed-species stand. *Journal of Hydrology* **400**, 244–254. doi:10.1016/j.jhydrol.2011.01.037.

Bassette, C. & Bussière, F. 2005 3-D modelling of the banana architecture for simulation of rainfall interception parameters. *Agricultural and Forest Meteorology* **129** (1–2), 95–100. doi:10.1016/j.agrformet.2004.11.004.

Bellot, J. & Escarre, A. 1998 Stemflow and throughfall determination in a resprouted Mediterranean holm-oak forest. *Annals of Forest Science* **55**, 847–865. doi:10.1051/forest:19980708.

Bouten, W., Heimovaara, T. J. & Tiktak, A. 1992 Spatial patterns of throughfall and soil water dynamics in a Douglas fir stand. *Water Resource Research* **28**, 3227–3233. doi:10.1029/92WR01764.

Brandt, C. J. 1989 The size distribution of throughfall drops under vegetation canopies. *Catena* **16**, 507–524. doi:10.1016/0341-8162(89)90032-5.

Carlyle-Moses, D. E., Laureano, J. F. & Price, A. G. 2004 Throughfall and throughfall spatial variability in Madrean oak forest communities of northeastern Mexico. *Journal of Hydrology* **297**, 124–135. doi:10.1016/j.jhydrol.2004.04.007.

Cattan, P., Bussière, F. & Nouvellon, A. 2007 Evidence of large rainfall partitioning patterns by banana and impact on surface runoff generation. *Hydrological Processes* **21**, 2196–2205. doi:10.1002/hyp.6588.

Cattan, P., Ruy, S. M., Cabidoche, Y. M., Findeling, A., Desbois, P. & Charlier, J. B. 2009 Effect on runoff of rainfall redistribution by the impluvium-shaped canopy of banana cultivated on an Andosol with a high infiltration rate. *Journal of Hydrology* **368**, 251–261. doi:10.1016/j.jhydrol.2009.02.020.

Crockford, R. H. & Richardson, D. P. 2000 Partitioning of rainfall into throughfall, stemflow and interception: effect of forest type, ground cover and climate. *Hydrological Processes* **14**, 2903–2920. doi:10.1002/1099-1085(200011/12).

CSY 2018 *China Statistical Yearbook*. China Statistics Press, Beijing, China.

Dezhban, A., Attarod, P., Amiri, Z. G., Pypker, T. G. & Nanko, K. 2019 Spatial and temporal variability of throughfall under a natural Fagus orientalis stand in the Hyrcanian forests, north of Iran. *Journal of Agricultural Science and Technology* **21**, 1843–1858. doi:jast.modares.ac.ir/article-23-24066.

Dou, B. Z. & Zhou, P. H. 1982 Measuring and calculating method of raindrop. *Bulletin of Soil and Water Conservation* **1**, 44–47. doi:10.13961/j.cnki.stbctb.1982.01.010.

Fan, J., Oestergaard, K. T., Guyot, A., Jensen, D. G. & Lockington, D. A. 2015 Spatial variability of throughfall and stemflow in an exotic pine plantation of subtropical coastal Australia. *Hydrological Processes* **29**, 793–804. doi:10.1002/hyp.10193.

Fathizadeh, O., Attarod, P., Keim, R. F., Stein, A., Amiri, G. Z. & Darvishsefat, A. A. 2014 Spatial heterogeneity and temporal stability of throughfall under individual Quercus brantii trees. *Hydrological Processes* **28**, 1124–1136. doi:10.1002/hyp.v28.3.

Germer, S., Elsenbeer, H. & Moraes, J. M. 2006 Throughfall and temporal trends of rainfall redistribution in an open tropical rainforest, south-western Amazonia (Rondônia, Brazil). *Hydrology Earth System and Science* **10**, 383–393. doi:hal.archives-ouvertes.fr/hal-00304865.

Gómez, J. A., Vanderlinden, K., Giráldez, J. V. & Fereres, E. 2002 Rainfall concentration under olive trees. *Agricultural Water Management* **55**, 53–70. doi:10.1016/S0378-3774(01)00181-0.

Hall, R. L. 2003 Interception loss as a function of rainfall and forest types: stochastic modelling for tropical canopies revisited. *Journal of Hydrology* **280**, 1–12. doi:10.1016/S0022-1694(03)00076-3.

Harris, D. 1997 The partitioning of rainfall by a banana canopy in St. Lucia, Windward Islands. *Tropical Agriculture* **74**, 198–202.

Holwerda, F., Scatena, F. N. & Bruijnzeel, L. A. 2006 Throughfall in a Puerto Rican lower montane rain forest: a comparison of sampling strategies. *Journal of Hydrology* **327**, 592–602. doi:10.1016/j.jhydrol.2005.12.014.

Isaaks, E. H. & Scrivastava, R. M. 1989 *An Introduction to Applied Geostatistics*. Oxford University Press, New York, USA.

Keim, R. F. & Link, T. E. 2018 Linked spatial variability of throughfall amount and intensity during rainfall in a coniferous forest. *Agricultural and Forest Meteorology* **248**, 15–21. doi:10.1016/j.agrformet.2017.09.006.

Keim, R. F., Skaugset, A. E. & Weiler, M. 2005 Temporal persistence of spatial patterns in throughfall. *Journal of Hydrology* **314**, 263–274. doi:10.1016/j.jhydrol.2005.03.021.

Klos, P. Z., Chain-Guadarrama, A., Link, T. E., Finegan, B., Vierling, L. A. & Chazdon, R. 2014 Throughfall heterogeneity in tropical forested landscapes as a focal mechanism for deep percolation. *Journal of Hydrology* **519**, 2180–2188. doi:10.1016/j.jhydrol.2014.10.004.

Kowalska, A., Boczoń, A., Hildebrand, R. & Polkowska, Z. 2016 Spatial variability of throughfall in a stand of Scots pine (*Pinus sylvestris* L.) with deciduous admixture as influenced by canopy cover and stem distance. *Journal of Hydrology* **538**, 231–242. doi:10.1016/j.jhydrol.2016.04.023.

Levia Jr, D. F. & Frost, E. E. 2006 Variability of throughfall volume and solute inputs in wooded ecosystems. *Progress in Physical Geography* **30**, 605–632. doi:10.1177/ 0309133306071145.

Levia, D. F., Nanko, K., Amasaki, H., Giambelluca, T. W., Hotta, N., Iida, S., Mudd, R. G., Nullet, M. A., Sakai, N., Shinohara, Y., Sun, X., Suzuki, M., Tanaka, N., Tantasirin, C. & Yamada, K. 2019 Throughfall partitioning by trees. *Hydrological Processes* **33**, 1698–1708. doi:10.1002/hyp.13432.

Lin, T. C., Hamburg, S. P., King, H. B. & Hsia, Y. 1997 Spatial variability of throughfall in a subtropical rain forest in Taiwan. *Journal of Environmental Quality* **26**, 172–180. doi:10.2134/jeq1997.00472425002600010025x.

Liu, W. J., Zhu, C. J., Wu, J. E. & Chen, C. F. 2016 Are rubber-based agroforestry systems effective in controlling rain splash erosion? *Catena* **147**, 16–24. doi:10.1016/j.catena.2016.06.034.

Liu, J. Q., Liu, W. J. & Zhu, K. 2018 Throughfall kinetic energy and its spatial characteristics under rubber-based agroforestry systems. *Catena* **161**, 113–121. doi:10.1016/j.catena.2017.10.014.

Liu, J. Q., Liu, W. J., Li, W. X. & Zeng, H. 2019 How does a rubber plantation affect the spatial variability and temporal stability of throughfall? *Hydrology Research* **50** (1), 60–70. doi:10.2166/nh.2018.028.

Lloyd, C. R. & Marques, A. O. 1988 Spatial variability of throughfall and stemflow measurements in Amazonian rainforest. *Agricultural and Forest Meteorology* **42**, 63–73. doi:10.1016/0168-1923(88)90067-6.

Loescher, H. W., Powers, J. S. & Oberbauer, S. F. 2002 Spatial variation of throughfall volume in an old-growth tropical wet forest, Costa Rica. *Journal of Tropical Ecology* **18**, 397–407. doi:10.1017/S0266467402002274.

Loustau, D., Berbigier, P., Granier, A. & Moussa, F. E. H. 1992 Interception loss, throughfall and stemflow in a maritime pine stand. I. Variability of throughfall and stemflow beneath the pine canopy. *Journal of Hydrology* **138**, 449–467. doi:10.1016/0022-1694(92)90130-N.

Lu, J. H., Yang, Z. H. & Zheng, X. K. 2015 Measuring of stain diameter and raindrop diameter with image processing method. *Journal of Jianghan University (Natural Science Edition)* **43**, 116–120. doi:10.16389/j.cnki.cn42-1737/n.2015.02.004.

Nanko, K., Hotta, N. & Suzuki, M. 2006 Evaluating the influence of canopy species and meteorological factors on throughfall drop size distribution. *Journal of Hydrology* **329**, 422–431. doi:10.1016/j.jhydrol.2006.02.036.

Nanko, K., Watanabe, A., Hotta, N. & Suzuki, M. 2013 Physical interpretation of the difference in drop size distributions of leaf drips among tree species. *Agricultural and Forest Meteorology* **169**, 74–84. doi:10.1016/j.agrformet.2012.09.018.

Rebelo, C. F. & Williamson, G. B. 1996 Driptips vis-à-vis soil types in central Amazônia. *Biotropica* **28** (2), 159–163.

Rodrigo, A. & Ávila, A. 2001 Influence of sampling size in the estimation of mean throughfall in two Mediterranean holm oak forests. *Journal of Hydrology* **243**, 216–227. doi:10.1016/S0022-1694(00)00412-1.

Sato, A. M., Avelar, A. D. & Netto, A. L. C. 2011 Spatial variability and temporal stability of throughfall in a eucalyptus plantation in the hilly lowlands of southeastern Brazil. *Hydrological Processes* **25**, 1910–1923. doi:10.1002/hyp.7947.

Song, Z. S., Steffen, S., Zhu, P. P., Philipp, G., Shi, X. Z. & Thomas, S. 2018 Spatial distribution of LAI and its relationship with throughfall kinetic energy of common tree species in a Chinese subtropical forest plantation. *Forest Ecology and Management* **425**, 189–195. doi:10.1016/j.foreco.2018.05.046.

Staelens, J., De Schrijver, A., Verheyen, K. & Verhoest, N. E. C. 2006 Spatial variability and temporal stability of throughfall water under a dominant beech (*Fagus sylvatica* L.) tree in relationship to canopy cover. *Journal of Hydrology* **330**, 651–662. doi:10.1016/j.jhydrol.2006.04.032.

Sun, X., Onda, Y., Chiara, S., Kato, H. & Gomi, T. 2015 The effect of strip thinning on spatial and temporal variability of throughfall in a Japanese cypress plantation. *Hydrological Processes* **29**, 5058–5070. doi:10.1002/hyp.10425.

Voss, S., Zimmermann, B. & Zimmermann, A. 2016 Detecting spatial structures in throughfall data: the effect of extent, sample size, sampling design, and variogram estimation method. *Journal of Hydrology* **540**, 527–537. doi:10.1016/j.jhydrol.2016.06.042.

Weiler, M. & Naef, F. 2003 An experimental tracer study of the role of macropores in infiltration in grassland soils. *Hydrological Processes* **17**, 477–493. doi:10.1002/hyp.1136.

Whelan, M. J. & Anderson, J. M. 1996 Modelling spatial patterns of throughfall and interception loss in a Norway spruce (*Picea abies*) plantation at the plot scale. *Journal of Hydrology* **186**, 335–354. doi:10.1016/S0022-1694(96)03020-X.

Wullaert, H., Pohlert, T., Boy, J., Valarezo, C. & Wilcke, W. 2009 Spatial throughfall heterogeneity in a montane rain forest in Ecuador: extent, temporal stability and drivers. *Journal of Hydrology* **377**, 71–79. doi:10.1016/j.jhydrol.2009.08.001.

Xu, X. Z., Zhang, H. W. & Zhu, M. D. 2004 Study on measuring method of particle size of raindrop and its improvement. *Soil and Water Conservation in China* **2**, 22–25. doi:10.14123/j.cnki .swcc.2004.02.010.

Yang, B., Zhang, W. J., Meng, X. J., Singh, A. K., Zakari, S., Song, L. & Liu, W. J. 2020 Effects of a funnel-shaped canopy on rainfall redistribution and plant water acquisition in a banana (*Musa spp.*) plantation. *Soil & Tillage Research* **203**, 104686. doi:10.1016/j.still.2020.104686.

Zhang, Y. F., Wang, X. P., Hu, R. & Pan, Y. X. 2016 Throughfall and its spatial variability beneath xerophytic shrub canopies within water-limited arid desert ecosystems. *Journal of Hydrology* **539**, 406–416. doi:10.1016/j.jhydrol.2016.05.051.

Zhang, W. J., Liu, W. J., Li, W. X., Zhu, X. A., Chen, C. F., Zeng, H. H., Jiang, X. J., Singh, A. K. & Yang, B. 2021 Characteristics of throughfall kinetic energy under the banana (*Musa nana* Lour.) canopy: the role of leaf shapes. *Catena* **197**, 104985. doi:org/10.1016/j.catena.2020.104985.

Zheng, J., Fan, J., Zhang, F., Yan, S. C., Wu, Y., Lu, J. S., Guo, J. J., Cheng, M. H. & Pei, Y. F. 2019 Throughfall and stemflow heterogeneity under the maize canopy and its effect on soil water distribution at the row scale. *Science of the Total Environment* **660**, 1367–1382. doi:10.1016/j.scitotenv.2019.01.104.

Zhu, C. J., Liu, W. J. & Wu, J. E. 2014 Rainfall erosivity and rainfall kinetic energy under rubber agroforestry system in Xishuangbanna. *Chinese Journal of Soil Science* **45**, 1218–1224. doi:10.19336/j.cnki.trtb.2014.05.032.

Zhu, X. A., Liu, W. J., Jiang, X. J., Wang, P. J. & Li, W. X. 2018 Effects of land-use changes on runoff and sediment yield: implications for soil conservation and forest management in Xishuangbanna, Southwest China. *Land Degradation & Development* **29** (9), 2962–2974. doi:10.1002/ldr.3068.

Zhu, X., He, Z. B., Du, J., Chen, L. F., Lin, P. F. & Tian, Q. Y. 2021 Spatial heterogeneity of throughfall and its contributions to the variability in near-surface soil water-content in semiarid mountains of China. *Forest Ecology and Management* **488**, 119008. doi:10.1016/j.foreco.2021.119008.

Zimmermann, A., Wilcke, W. & Elsenbeer, H. 2007 Spatial and temporal patterns of throughfall quantity and quality in a tropical montane forest in Ecuador. *Journal of Hydrology* **343**, 80–96. doi:10.1016/j.jhydrol.2007.06.012.

First received 4 March 2021; accepted in revised form 26 July 2021. Available online 26 August 2021